Available online at www.sciencedirect.com
ScienceDirect
Journal of Catalysis 244 (2006) 65–77
JOURNAL OF CATALYSIS
www.elsevier.com/locate/jcat

A density functional theory study of the alkylation of isobutane with butene over phosphotungstic acid

Michael J. Janik [a], Robert J. Davis [a], Matthew Neurock [a,b,*]

[a] *University of Virginia, Department of Chemical Engineering, 102 Engineers' Way, Charlottesville, VA 22904, USA*
[b] *University of Virginia, Department of Chemistry, McCormick Road, Charlottesville, VA 22904, USA*

Received 20 June 2006; revised 3 August 2006; accepted 8 August 2006

Available online 28 September 2006

Abstract

The deactivation of solid acid catalysts during the alkylation of isobutane with butene has significantly impeded replacement of the commonly used homogeneous catalysts. The relative rates of alkylation and hydride transfer control the rate of heavy hydrocarbon buildup, leading to blocking of catalyst pores and acid sites. Herein the mechanisms of hydride transfer and alkylation over phosphotungstic acid are examined using ab initio density functional theory methods. The transition state of hydride transfer is a carbenium ion, with shared-hydride carbonium ions representing lower energy intermediates. Although the transition state for the alkylation step is also a carbenium ion, it is stabilized by interaction with the alkene reactant. Therefore, the barrier for alkylation is intrinsically lower than that for hydride transfer, thus providing a favorable path to the buildup of heavy hydrocarbons on the acid surface. The implications of these findings on the design of effective catalysts for alkylation are discussed.

Keywords: Heteropolyacid; Polyoxometalate; HPA; Alkylation; Solid acid; Hydride transfer; Deactivation; DFT; Quantum chemical

1. Introduction

Acid catalysis is at the heart of many hydrocarbon conversion processes including catalytic cracking, isomerization, oligomerization, and alkylation. The first three of these processes are typically carried out over solid acids, whereas the alkylation of isobutane with butene is carried out using mainly homogeneous HF and H_2SO_4, which are highly corrosive and entail waste disposal and catalyst separation issues. Despite nearly 30 years of research [1–3], the commercialization of solid acid alternatives for alkylation is limited. Catalyst deactivation remains the foremost challenge in finding acceptable solid acid replacements. To advance our efforts toward the design of new solid acid catalysts, a more complete understanding of the fundamental structural and electronic features that control catalyst acidity, selectivity, and potential modes of deactivation is required. Although numerous studies have been devoted to elucidating the operative mechanisms for solid acid-catalyzed conversion processes, our understanding remains fragmented and rather incomplete. Over the past decade, however, theoretical efforts have helped establish the reaction mechanisms of many hydrocarbon conversion processes over acidic zeolites. Herein we extend that work using quantum mechanical methods to examine the energetics of key reaction steps for alkylation over heteropolyacids (HPAs).

Alkylate produced from the C_4 byproducts of a catalytic cracking unit is used as a high octane (octane number ∼95) blending stock for gasoline. The worldwide alkylation production capacity exceeds 1.9 million barrels per day [4]. The alkylation of isobutane with butene occurs via a complex reaction network that produces a broad distribution of products. The desired products are highly branched C_8 alkanes, mainly trimethylpentanes (TMPs). A simplified mechanism for solid acid-catalyzed alkylation is illustrated in Fig. 1 [2,5]. Alkylation is initiated by the adsorption of butene (reaction 1). This is followed by hydride transfer from isobutane to the adsorbed *s*-butyl species to produce an adsorbed *t*-butyl intermediate and an *n*-butane molecule (reaction 2). The adsorbed *t*-butyl in-

* Corresponding author.
E-mail address: mn4n@virginia.edu (M. Neurock).

0021-9517/$ – see front matter
doi:10.1016/j.jcat.2006.08.013

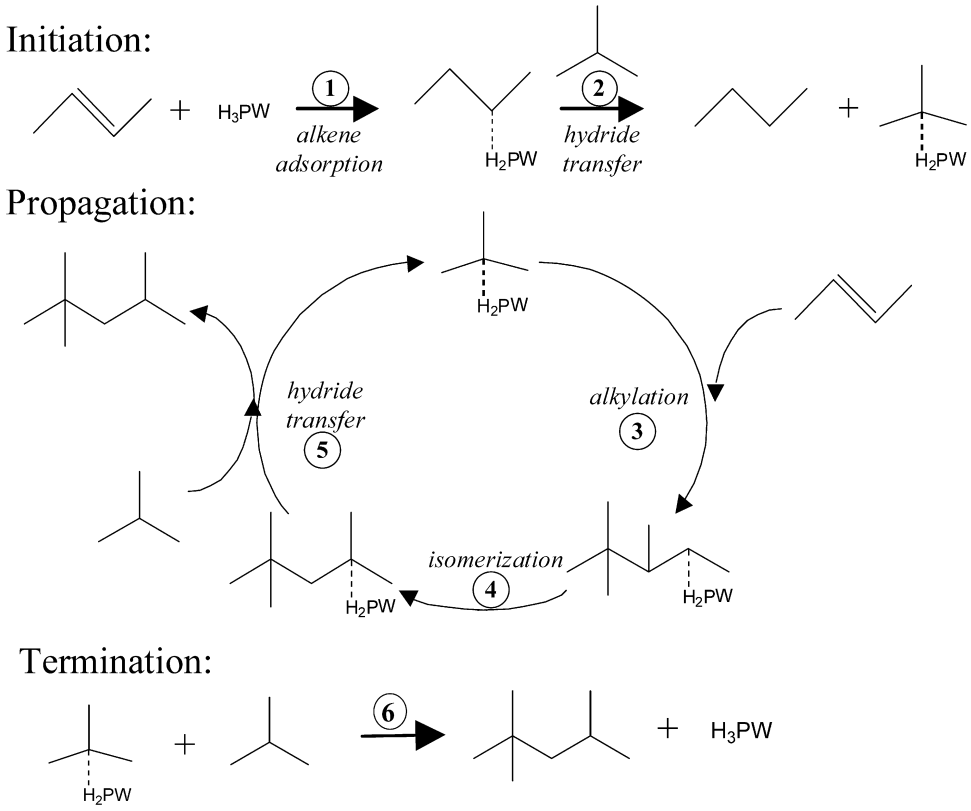

Fig. 1. The mechanism of the alkylation of isobutane and *n*-butene over phosphotungstic acid ($H_3PW_{12}O_{40}$, abbreviated H_xPW). There is no implication as to the nature of the adsorbed alkyl species, and the catalyst is included only to indicate the involvement of the catalytic site.

termediate initiates the propagation cycle. A butene molecule reacts with the *t*-butyl intermediate to form adsorbed 2,2,3-trimethylpentane (2,2,3-TMP) (reaction 3). The adsorbed 2,2,3-TMP can subsequently isomerize through hydride and methyl shifts (e.g., reaction 4). A fluid-phase isobutane molecule can react with the adsorbed C_8 species via hydride transfer to generate the C_8 alkane product and regenerate the adsorbed *t*-butyl intermediate, which closes the cycle (reaction 5). Termination of the cycle occurs through a sequence typically termed "self-alkylation" (reaction 6) in which an adsorbed *t*-butyl species desorbs as isobutene, which can then alkylate with a second adsorbed *t*-butyl species.

Competing reactions produce undesired side products that ultimately lead to catalyst deactivation. The C_8 species can desorb as an alkene and subsequently alkylate an adsorbed *t*-butyl species rather than undergo hydride transfer. The adsorbed C_8 species can combine with another butene molecule to produce an adsorbed C_{12} species, which can further react. Skeletal isomerization and β-scission reactions lead to a wide distribution of products. Alkene oligomerization can also occur, leading to the production of C_8 alkenes or other heavier hydrocarbons. Heavy hydrocarbons may plug catalyst pores or block active catalyst sites, leading to deactivation. Ideally, hydride transfer from isobutane to the adsorbed C_8 species occurs before further alkylation or alkene desorption, thus terminating the growing chain and preventing heavy hydrocarbon buildup. However, the alkylation step is estimated to occur at a rate two to three orders of magnitude faster than hydride transfer [6,7], and the formation of multiple alkylates (C_{12} and greater) is directly tied to catalyst deactivation [6]. Deactivated zeolite catalysts contain large amounts of heavy hydrocarbons [8], and only recently has an industrial process, with the catalyst taken off-line and regenerated every 1–3 h, become economical [9,10]. Alkylation is performed industrially in extreme excess of isobutane over butene to maximize the relative hydride transfer rate [1,11].

Zeolites have a high initial activity for alkylation; however, both the activity and the selectivity to C_8 alkanes decrease with time on stream [2,6,7,12,13]. As the olefin conversion decreases, the fraction of higher alkenes in the product stream typically increases, and at long reaction times, only butene oligomerization is catalyzed. This indicates that at long reaction times, the hydride transfer step ceases, and thus the loss of activity and selectivity is assumed to result from a decreased ability to promote the hydride transfer step [2,6,14–16]. Understanding the mechanism for acid-catalyzed hydride transfer has thus been proposed as "mandatory for the rational search for improved solid catalysts" for this reaction [2]. The determination of the reaction mechanism, including the transition state(s) for the hydride transfer step over acid catalysts, will help elucidate the requirements of the active site for hydride transfer. The relative rate of hydride transfer compared with alkylation and isomerization must be considered in the rational design of effective catalytic materials.

Theoretical studies of hydrocarbon conversion has been used to elucidate the important properties of zeolite catalysts for these processes. Whereas the active intermediate for conver-

sions in liquid acids is a carbenium ion [11,15], theoretical studies indicate that carbenium ions are transition states on the zeolite surface [17,18]. The lowest energy adsorbed state of an alkyl species on a zeolite is an alkoxide [19,20], in which a covalent bond is formed between an oxygen atom of the zeolite and a carbon atom of the alkyl species; however, the transition states for alkene adsorption [21–27] and alkylation/β-scission reactions [18,28] are carbenium ions. Theoretical studies of hydride transfer over solid acid catalysts are limited but have identified a carbonium intermediate along the reaction coordinate in which a two-electron C–H–C bond is formed [17,18, 29–31]. Questions remain as to what is required of an acid site to promote hydride transfer, with various researchers proposing that acid site density [13,15,32,33], acid site strength [15], site homogeneity [13], proton mobility [34], or site-specific sterics [6] control the rate of hydride transfer.

An alternative to zeolite catalysts, heteropolyacids (HPAs) have the ability to catalyze isobutane/butene alkylation. HPAs are proposed to be superacids [35,36], and their acid strength has stimulated interest in their use as alkylation catalysts. Phosphotungstic acid ($H_3PW_{12}O_{40}$ [HPW]), supported on a high-surface area silica support [37,38] or as a partially alkaline salt [39,40], shows a high initial rate for the alkylation of isobutane with butene. However, it deactivates rapidly with time on stream. The ability to tune the acid and redox properties by altering the chemical composition or the physical properties by changing the counter-cation or catalyst support make HPAs an attractive solid acid alternative for alkylation. Fundamental studies of key reaction steps and the requirements of the catalytic site are necessary to guide the development of HPA catalysts. We previously used quantum chemical methods to study the adsorption of alkenes [41,42] and the stability of carbenium ions [43] on HPW. In the present study, we used density functional theory (DFT) methods to explore the mechanisms of hydride transfer and alkylation on HPW.

2. Computational methods

Periodic DFT as implemented in the Vienna ab initio Simulation Package (VASP) [44–46] was used to identify equilibrium and transition state structures and their corresponding energetics. All calculations were performed with ultrasoft pseudopotentials to describe electron–ion interactions [47] and the Perdew–Wang (PW91) form of the generalized gradient approximation for the exchange and correlation energies [48]. A cutoff energy of 396.0 eV for the plane-wave basis set was used in all calculations. The Brillouin zone sampling was restricted to the Γ-point [49]. The molecular system was represented within the periodic code by surrounding the species with vacuum in a $20 \times 20 \times 20$ Å^3 supercell. Convergence with respect to cell size was confirmed to within 5 kJ mol^{-1} for the adsorbed t-butyl alkoxide and carbenium ion species. Full geometry optimizations were performed for each structure until the forces on each atom were <0.05 eV Å^{-1}. These methods have previously been shown to calculate an equilibrium geometry of the phosphotungstic acid Keggin structure, in agreement with experimental data [50].

Transition states were located using the nudged elastic band (NEB) method as implemented in VASP [51]. This method involves optimizing a chain of images that connect the reactant and product states to determine the minimum energy reaction path. The nuclear positions are optimized with the constraint of moving only perpendicular to the current hypertangent, defined as the normal vector between the two neighboring images. The transition state was identified as the image with the highest energy, an absolute tangential force <0.05 eV Å^{-1}, and a change in the sign of the tangential force across the adjacent images. Transition states were optimized separately following the NEB calculation such that all atomic forces were <0.05 eV Å^{-1}.

In this work, the highest energy structures located along the reaction coordinate were typically tertiary carbenium ions. Their nature as intermediates or transition states was not confirmed through vibrational analysis, even though we refer to them as transition states. The reaction coordinate for hydride transfer over zeolites is known to be extremely flat, making it difficult to isolate the true transition state [18]. We have previously shown that tertiary carbenium ions are both transition states and meta-stable intermediates over HPW and that the potential energy surface (PES) for displacement of the intermediates is extremely flat [43]. The carbenium-ion transition states and intermediates were within 6 kJ mol^{-1} in energy, and the imaginary frequency at the transition state between the carbenium ion and alkoxide was $88i$ cm^{-1}. Furthermore, both equilibrium and transition states within the structural convergence criteria used indicate low-frequency imaginary modes for methyl rotations unrelated to the reaction chemistry. The anharmonicity of these modes is expected to be large and, therefore, the calculated harmonic frequency is extremely sensitive to the displacement used in calculating the Hessian [52]. The flat PES and difficulties dealing with the methyl rotational modes make isolation and confirmation of transition states through vibrational analysis very tedious and somewhat impractical, requiring large amounts of computational time.

We also previously showed that the harmonic oscillator approximation does not hold in the ground vibrational state for displacements of the tertiary carbenium ion relative to the catalyst surface [43]; therefore, we do not report ZPVE corrections here. Because of the flat nature of the PES (little change in energy with large structural changes) along the hydride transfer coordinate, the relative energies reported in this study may be considered within the accuracy of the generalized gradient DFT approach; however, the molecular geometries may not represent the exact extrema.

2.1. Choice of initial and final adsorbed states and reaction coordinates

Hydride transfer involves the shift of a hydride (H^-) from a fluid-phase isobutane to the adsorbed alkyl fragment. The relative rate of hydride transfer to an adsorbed C_8 alkyl species controls catalyst deactivation during alkylation. Furthermore, hydride transfer to a tertiary carbon is much faster than to a secondary carbon atom, as evidenced by the fact that all C_5–C_{14} alkanes produced during alkylation contain a tertiary carbon

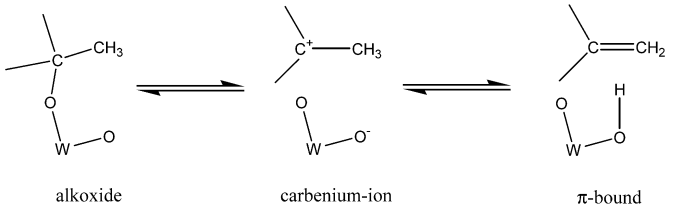

Scheme 1. The proposed mechanism for conversion of an adsorbed *t*-butyl species between adsorbed states over phosphotungstic acid. The tungsten-oxide fragment represents a section of the Keggin unit.

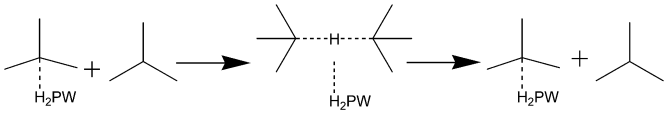

Scheme 2. The proposed mechanism of hydride transfer includes the formation of an intermediate in which the hydride is shared in a 2 electron, C–H–C bond.

atom [5]. To better understand the factors that control hydride transfer, we examine transfer from isobutane to both a secondary and a tertiary carbon atom. To model hydride transfer to a tertiary carbon atom, we examined the degenerative reaction of hydride transfer from isobutane to an adsorbed *t*-butyl intermediate. The transfer of a hydride from isobutane to an *s*-butyl intermediate was used to model transfer to a secondary carbon atom.

We compare the activation barrier associated with the alkylation step with that of the hydride transfer reaction. The alkylation of an adsorbed C_8 species with an additional alkene molecule leads to heavy hydrocarbon buildup. To minimize the computational requirements, we substituted the adsorbed C_8 species with a model C_4 surface intermediate and thus examined the alkylation of two C_4 species. Alkylation of adsorbed *s*-butyl and *t*-butyl species with *trans*-2-butene were examined. The alkylation of an adsorbed *s*-butyl species with *trans*-2-butene is the key step in acid-catalyzed butene dimerization and represents alkylation of a secondary carbon atom within the overall alkylation mechanism.

Multiple adsorbed states exist for an alkyl species bound to HPW [41,42]. The conversion among adsorbed states is illustrated in Scheme 1. An adsorbed alkyl species on the HPW surface, although not necessarily formed through alkene adsorption, has the same number of each atom type as the separated alkene and HPW species. To provide consistent reference energy between hydride transfer and alkylation processes, all energies are given relative to separated alkene, alkane, and HPW species. The ground state for an adsorbed alkene, or surface alkyl species, is an alkoxide. A second adsorbed state, referred to as the π-bound state, is characterized by the interaction of the electron density from a C=C double bond with the surface hydroxyl through formation of a hydrogen bond. The transition state between the two adsorbed states is a carbenium ion, in which the proton is donated to one carbon atom of the alkene double bond and a positive charge is localized on the other carbon atom. For a tertiary alkyl species, a carbenium ion also represents a meta-stable intermediate over HPW. Although the alkoxide has been experimentally confirmed to be the most populous adsorbed alkyl species [19,20], Boronat et al. [30] found that hydride transfer between propane and an adsorbed propyl species can occur to a π-bound state on a zeolite. Moreover, Svelle et al. [53] found that alkene dimerization can occur either directly from the π-bound state (concerted mechanism) or through formation of the alkoxide and subsequent coupling with the alkene (stepwise mechanism). Therefore, we examined hydride transfer and alkylation with the adsorbed alkyl species initially in both the π-bound or alkoxide state and directly from the *t*-butyl carbenium intermediate.

We also postulate, along with other researchers [17,18,29–31], that a shared-hydride intermediate exists along the hydride transfer reaction coordinate, in which a two-electron C–H–C bond is formed (Scheme 2); however, the position of this intermediate on the catalyst surface is not implied here. The formation of this intermediate rules out surface-mediated hydride transfer, in which isobutane is first activated to form a surface hydrogen and an adsorbed alkyl species (thereby reducing the HPA), followed by addition of a hydride to the adsorbed alkyl group (oxidizing the HPA). Although the dissociative adsorption of isobutane is thermoneutral over HPW, a high activation barrier (on the order of $\sim$200 kJ mol^{-1} based on comparisons with similar systems [54]) is expected because the interaction of isobutane with the surface oxygen atoms is repulsive at short distances. Therefore, activation of isobutane by the Keggin unit before hydride transfer is not a kinetically viable path.

The choice of initial and final state configurations dictates the reaction path considered within the NEB transition state search. Because the reaction occurs over a multidimensional flat PES, the search method may not isolate the global minimum energy path. Therefore, transition state searches for the hydride transfer reaction were performed over various sections of the Keggin unit and between multiple equilibrium structures. The alkoxide is taken to reside on a terminal oxygen atom (O_d) of the HPW Keggin unit, which has been shown to be the lowest energy structure [41]. Because rotation of the adsorbed alkoxide about the W–O_d bond is facile, multiple reaction trajectories were considered, starting from the alkoxide. The π-bound adsorbed state is assumed to involve a proton on a bridging O_c atom, because this is the energetically preferred proton location [50]. The PES for movement of the shared-hydride intermediate over the HPW surface is also extremely flat, and thus multiple positions for the formation of this intermediate were considered.

Although we would expect the approach of isobutane or *trans*-2-butene to the catalyst surface to be weakly exothermic, the DFT calculated interaction energy for the initial approach to the adsorbed alkyl species on HPW is thermoneutral. This is expected because DFT does not appropriately treat the dispersion forces responsible for the initial weak attractive interaction [55]. However, the magnitude of these interactions is not expected to vary substantially among C_4 species or reaction steps, and thus analysis of relative barriers is reasonable. Equilibrium structures were located with isobutane near the adsorbed alkyl species, with the approach angle chosen such that the subsequent hydride transfer reaction coordinate was well defined. Multiple transition state searches

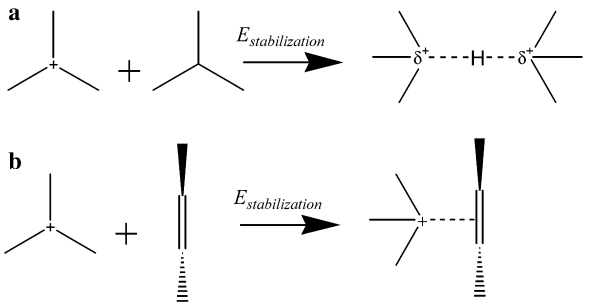

Scheme 3. A gas-phase *t*-butyl carbenium ion is stabilized by (a) isobutane through the formation of a shared-hydride species or (b) *trans*-2-butene through interaction with the C=C double bond.

were then performed between the different "initial" structures with isobutane near the adsorbed alkyl species and "final" shared-hydride intermediates placed at various positions. Hydride transfer was then completed by the antisymmetric dissociation of the shared-hydride intermediate. Generally the lowest energy reaction paths are those that keep the transition state and shared-hydride intermediates closest to the HPW surface. Only the paths with the lowest energy transition states are discussed in detail here.

The alkylation step proceeds via the approach of *trans*-2-butene to the adsorbed alkyl species. The two C_4 fragments subsequently couple to form a C_8 carbenium ion, which can then adsorb to the surface as an alkoxide. The transition states were located along the reaction coordinate over the area of HPW that gave the lowest hydride transfer barrier, thereby allowing direct comparison of the barriers of the two steps.

3. Results and discussion

3.1. Gas-phase hydride transfer and alkylation

Before examination of acid-catalyzed hydride transfer and alkylation, the interaction of carbenium ions with isobutane and *trans*-2-butene was examined in the gas phase. Previous ab initio studies showed that hydride transfer between a *t*-butyl carbenium ion and isobutane occurs in the gas phase through exothermic formation of a two-electron C–H–C bond, as illustrated in Scheme 3a followed by antisymmetric dissociation [56–58].

The alkylation of a butyl carbenium ion with an alkene in the gas phase produces a C_8 carbenium ion. However, local minimum energy structures were located in which the carbenium ion was stabilized by its interaction with the electron density of the C=C double bond (Scheme 3b), and the energies of these structures were only slightly higher than those of the C_8 carbenium ions. These structures are proposed as intermediates in the alkylation reaction, and their energies and structures are used to provide a comparison between the interaction of carbenium ions with alkanes and alkenes.

To provide a comparison with the energies over the HPW surface, the structure and energy of the gas-phase intermediates were determined. The stabilization energy, $E_{\text{stabilization}}$, of the carbenium ion by isobutane or *trans*-2-butene is the energy released when the carbenium ion is stabilized by interaction with the neutral hydrocarbon, defined as

$$E_{\text{stabilization}} = E_{\text{intermediate}} - E_{\text{carbenium}} - E_{\text{alkene/alkane}}, \qquad (1)$$

where $E_{\text{carbenium}}$ is the energy of the gas-phase carbenium ion, $E_{\text{alkene/alkane}}$ is the energy of the stabilizing molecule, and $E_{\text{intermediate}}$ is the energy of the shared-hydride or alkene-stabilized intermediate. The stabilization energy for a *t*-butyl carbenium ion is $-49\ \text{kJ mol}^{-1}$ by isobutane (structure **A**, Fig. 2a) and $-48\ \text{kJ mol}^{-1}$ by *trans*-2-butene (structure **B**, Fig. 2a). The stabilization energy for a *s*-butyl carbenium ion is $-83\ \text{kJ mol}^{-1}$ by isobutane (structure **C**, Fig. 2b) and $-104\ \text{kJ mol}^{-1}$ by *trans*-2-butene (structure **D**, Fig. 2b). The alkene-stabilized intermediates are similar to cyclopropyl cations; however, the C=C double bond is only slightly elongated (1.36 Å for *t*-butyl stabilization and 1.38 Å for *s*-butyl stabilization) from its equilibrium distance in isolated *trans*-2-butene (1.34 Å). Structural and atomic charge analyses (see supplementary material) indicate that the positive charge of the carbenium ion is distributed between fragments after stabilization and that the unsaturated carbon atom adopts an intermediate hybridization between sp^2 and sp^3.

A series of constrained optimizations was performed to elucidate the distance-dependent interactions between the carbenium ions and the neutral hydrocarbons. For the interaction with isobutane, the C–C distance across the shared hydride was incrementally increased. For the interaction with *trans*-2-butene, the distance between the unsaturated carbon of the carbenium ion and the C=C double bond of the alkene was incrementally increased. Fig. 2a shows the optimized intermediate structures and stabilization energy as a function of the distance from the optimum position for the *t*-butyl carbenium ion. Fig. 2b illustrates the stabilization of the *s*-butyl carbenium ion as a function of distance. For the *s*-butyl/isobutane complex, there are two local minimum energy structures for C–C distances >2.9 Å, with the shared-hydride closer to either the *s*-butyl or *t*-butyl fragments. Only the energy of the less-stable local minimum, with the hydride closer to the *t*-butyl species, is reported here, to represent stabilization of the *s*-butyl cation by isobutane. For C–C distances <2.9 Å, only a single minimum with the hydride closer to the *s*-butyl species was identified. The minimum energy structure for stabilization of the *s*-butyl by *trans*-2-butene occurs with the two fragments significantly closer than for stabilization of the *t*-butyl species.

The stabilization energy as a function of distance from the equilibrium position asymptotically approaches zero as the two fragments move farther apart, indicating that dissociation of the intermediate complexes is unactivated. However, interaction with the alkene is substantially longer-range due to the diffuse electron density of the C=C double bond. Furthermore, the interaction with isobutane is directional, requiring a fairly linear C–H–C bond, whereas translation of the alkene along the C=C vector weakens the interaction energy only slightly.

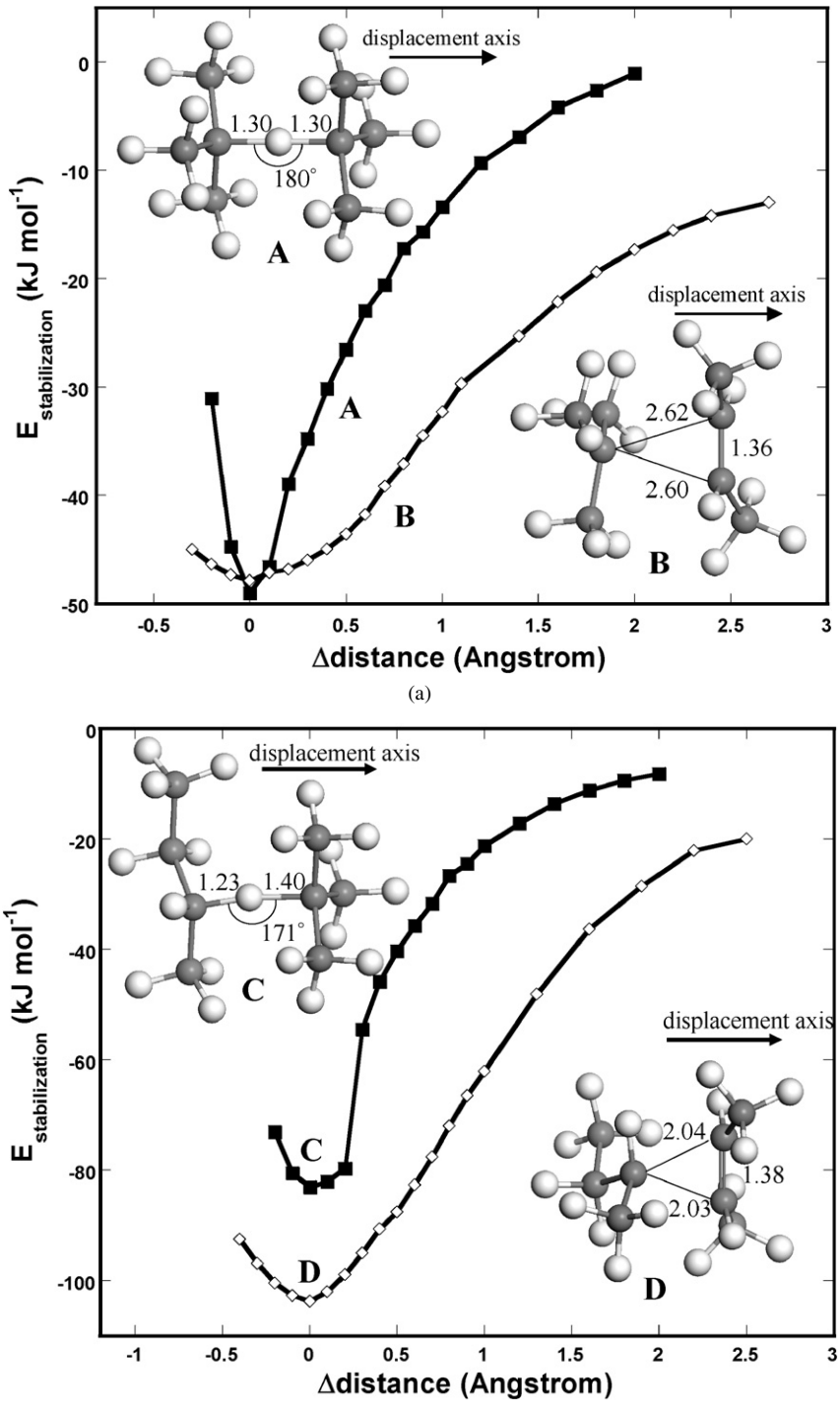

Fig. 2. Carbenium ions are stabilized in the gas phase by both alkanes or alkenes. (a) A *t*-butyl carbenium is stabilized by (**A**) isobutane through formation of a shared-hydride complex or (**B**) *trans*-2-butene by interaction of the unsaturated carbon atom with the alkene double bond. (b) A *s*-butyl carbenium ion is stabilized by (**C**) isobutane through formation of a shared-hydride complex or (**D**) *trans*-2-butene by interaction of the unsaturated carbon atom with the alkene double bond. Structures shown represent the energy minimum of the intermediate; data are plotted as a function of the distance in which the stabilizing species is displaced. Distance labels are in Å.

3.2. HPW-catalyzed hydride transfer from isobutane to an adsorbed t-butyl intermediate

The minimum energy path for hydride transfer from isobutane to an adsorbed *t*-butyl species occurs over the O_d–W–O_c region of the HPW Keggin unit. This area of the surface allows the positively charged alkyl species to interact with multiple oxygen atoms at the exterior surface, leading to greater charge stabilization. Comparisons with different reaction trajectories over the surface are presented after a discussion of the minimum energy path. A reaction coordinate diagram and key structures for the formation of the shared-hydride intermediate are shown

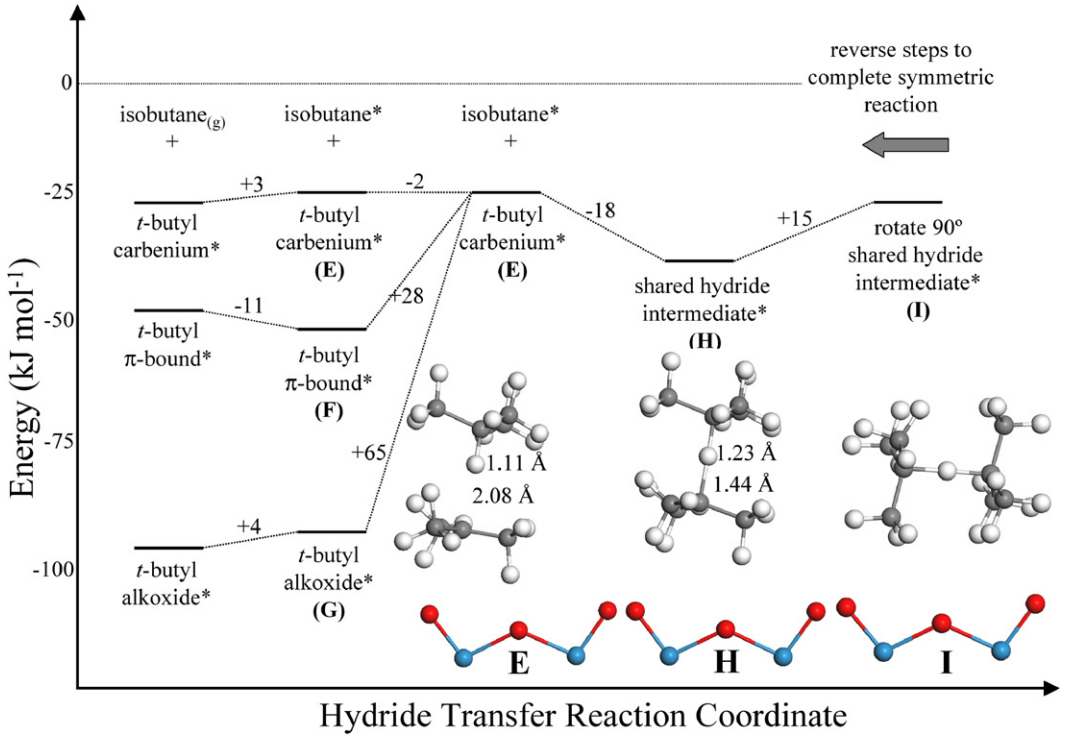

Fig. 3. Reaction energy diagram for hydride transfer from isobutane to an adsorbed t-butyl species over HPW. Energies are given relative to separated isobutene, isobutane, and $H_3PW_{12}O_{40}$ fragments. Asterisks label surface species. Key structures are illustrated. All structures are illustrated and detailed in supplementary material. All calculations were performed on the full Keggin unit, as illustrated for structure **E** in Fig. 4.

in Fig. 3, and a full view of the key transition state structure and atom labels is provided in Fig. 4. Additional structures and interatomic distances are provided in supplementary materials. Hydride transfer was examined with the t-butyl species initially in the alkoxy, π-bound, and carbenium-ion adsorbed states. In each case, the maximum in energy along the reaction coordinate is a tertiary carbenium ion that has little interaction with the nearby isobutane molecule.

The initial approach of isobutane to the adsorbed alkyl species is approximately thermoneutral, with isobutane positioned such that the tertiary carbon of the adsorbed t-butyl species is linear with the tertiary C–H bond of isobutane. The optimized initial states with isobutane nearby are labeled **E** for the carbenium ion, **F** for the π-bound state, and **G** for the alkoxide. The optimized intermediate in which the hydride is shared between the t-butyl species and isobutane over the same area of the Keggin unit is labeled structure **H**. In this structure, the t-butyl carbenium ion is stabilized by -13 kJ mol^{-1} compared with the separated isobutane and surface t-butyl carbenium ions. This stabilization energy is substantially lower than that for the gas-phase carbenium ion (-49 kJ mol^{-1}), because the positive charge is already partially stabilized by the Keggin unit. In the intermediate structure (**H**), the alkyl fragment—and thereby the positive charge—are lifted away from the surface (increase in W–O_d from 2.82 in **E** to 3.84 in **H**), weakening the Coulombic interaction with the anionic surface to facilitate stabilization by the alkane. The shared hydride remains closer to the isobutane species [C(3i)–H$^-$ = 1.23 Å] than to the t-butyl group [C(3t)–H$^-$ = 1.44 Å] such that the positive charge is

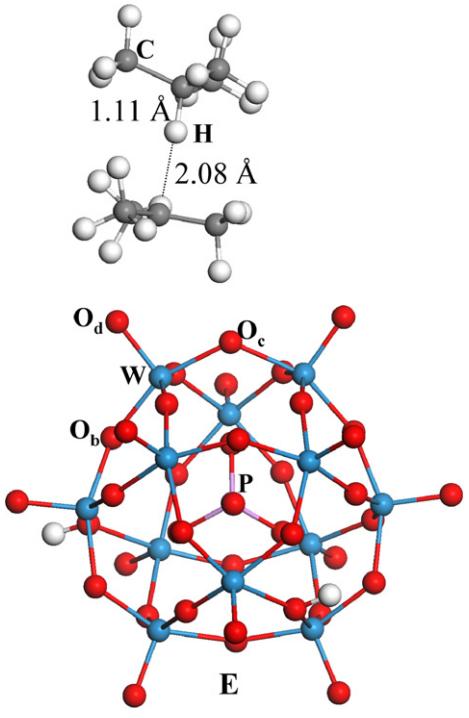

Fig. 4. The structure of the highest energy transition state for hydride transfer from isobutane to an adsorbed t-butyl species over phosphotungstic acid. This structure represents the transition state, regardless of whether the initial adsorbed t-butyl species is in the alkoxy or π-bound state. Progression along the hydride transfer coordinate subsequently forms an intermediate in which the labeled H atom is shared between the two tertiary carbon atoms in a linear, C–H–C bond.

partially segregated toward the Keggin unit surface. The C–C–C–$C_{tertiary}$ dihedral angles indicate hybridization between sp^2 and sp^3 for each of the tertiary carbon atoms, with the *t*-butyl species (20°) closer to planar than isobutane (27°). The closest methyl hydrogen–oxygen distances are 2.3–2.6 Å, suggesting that a weak interaction between the Keggin surface and the hydrogen may be present; however, the major interaction with the surface is Coulombic.

The conversion of the carbenium ion intermediate (**E**) to the shared-hydride intermediate (**H**) is unactivated. The NEB transition state search between the alkoxide (**G**) and intermediate (**H**) locates a transition state (**E′**) similar in geometry and energy (2 kJ mol^{-1} less stable) to structure **E**. Optimization of the transition state with the isobutane molecule removed does not perturb the carbenium ion structure, indicating that the interaction energy between isobutane and the *t*-butyl fragment is very small. Similarly, the transition state search between the π-bound state (**F**) and the shared-hydride intermediate located a *t*-butyl carbenium ion (**E″**) as the energy maximum, with little or no interaction between the *t*-butyl fragment and isobutane. This structure was 2 kJ mol^{-1} more stable than structure **E**, with the only significant structural difference being a slightly shorter O_c–H distance. These results indicate that the transition state for hydride transfer to an adsorbed *t*-butyl species is a *t*-butyl carbenium ion (**E**) that is independent of the starting adsorbed state. Furthermore, the isobutane molecule does not participate in the conversion of the adsorbed *t*-butyl species from the alkoxide or π-bound state into a carbenium ion. The energy of the transition state varies slightly (±2 kJ mol^{-1}) in the nudged elastic band calculation with the use of different initial and final states. Only the energy of the transition state located for the transformation of the alkoxide is given in Fig. 3 (and subsequent reaction energy diagrams) to provide a consistent comparison between competing elementary reactions. The activation barrier for formation of the shared-hydride intermediate is 28 kJ mol^{-1} from the π-bound state and 69 kJ mol^{-1} from the alkoxide.

To complete the hydride transfer process, the shared-hydride intermediate must rotate on the HPW surface so that the *t*-butyl group that began as isobutane is closer to the surface. An intermediate of this rotation, in which the C–H–C bond is rotated 90° in the plane of Fig. 3, is labeled structure **I**. Structure **I** is 15 kJ mol^{-1} less stable than structure **H**, indicating that rotation of the shared-hydride structure may affect the overall hydride transfer rate. The rotation was not examined in detail because it occurs over an extremely flat PES, and multiple interactions between methyl hydrogen atoms and surface oxygen atoms are possible. Because small perturbations to the position of the shared-hydride intermediate lead to only slight changes in energy, the predominant barrier for hydride transfer is the formation of the initial *t*-butyl carbenium ion (state **E**). Weak stabilization of the *t*-butyl carbenium ion by isobutane may allow for multiple dissociation/formation steps along the reaction path. After rotation, the degenerative isobutane-to-*t*-butyl hydride transfer is completed by the reverse of the intermediate formation steps. Despite the flat PES for movement of the shared-hydride intermediate over the HPW surface, there is a strong Coulombic interaction preventing desorption. An energy input of 226 kJ mol^{-1} is necessary to convert the shared-hydride intermediate (**H**) to a gas-phase cationic shared-hydride species (**A**) and the anionic $H_2PW_{12}O_{40}^{1-}$ species.

Table 1
Relative energies (RE) of carbenium-ion transition states and shared-hydride intermediate for isobutane to *t*-butyl hydride transfer over various areas of the HPW surface

Hydride transfer area	RE[a] (kJ mol^{-1})	
	TS	Shared H^-
O_d–W–O_c plane	0	−16
O_d–W–O_b plane	+37	0
Above O_d	+17	+1
Between W_3O_9 trimers	+29	+5

[a] Energy is relative to separated isobutane, isobutene, and $H_3PW_{12}O_{40}$ species.

Multiple reaction trajectories were explored for hydride transfer to the *t*-butyl alkoxide over HPW. Formation of the shared-hydride intermediate was considered over the O_d–W–O_b plane, directly over an O_d atom, and over an open area of the Keggin structure between W_3O_9 trimers. In all cases, *t*-butyl carbenium ions were found to be transition states, with no interaction between the carbenium ion and isobutane. The energies of the carbenium-ion transition states and shared-hydride intermediates over different areas of the Keggin unit are given in Table 1.

Similar studies performed on zeolitic clusters have suggested that the shared-hydride structure represents the transition state for hydride transfer [17,29], or that the energy of the transition state is close to that of the shared hydride [18,30,31]. Our results differ qualitatively, whereas for each reaction coordinate examined herein, a higher-energy carbenium-ion transition state is located before formation of the stabilized complex. However, the energy of stabilization is small, and the energy of the shared-hydride structure depends on its position and orientation over the surface. Therefore, the possibility that the shared-hydride intermediate must occupy a higher energy structure along the reaction coordinate cannot be ruled out.

3.3. HPW-catalyzed hydride transfer from isobutane to an adsorbed s-butyl intermediate

The reaction energy diagram and key structures for formation of the shared-hydride intermediate from an adsorbed *s*-butyl species and isobutane over the O_d–W–O_c area of HPW is illustrated in Fig. 5. Similar to the isobutane-to-*t*-butyl hydride transfer, the conversion of the adsorbed state to a secondary carbenium ion is the rate-limiting step for the isobutane-to-*s*-butyl hydride transfer. The secondary carbenium ion is less stable, and thus the activation barriers for formation of the shared-hydride intermediate are greater: 48 kJ mol^{-1} from the π-bound state and 85 kJ mol^{-1} from the alkoxide. The overall reaction, converting an *s*-butyl alkoxide and isobutane to a *t*-butyl alkoxide and *n*-butane, is exothermic by −14 kJ mol^{-1}.

Hydride transfer from isobutane to an adsorbed *s*-butyl species also progresses through a shared hydride intermediate. The rotation of this intermediate is slightly exothermic, again

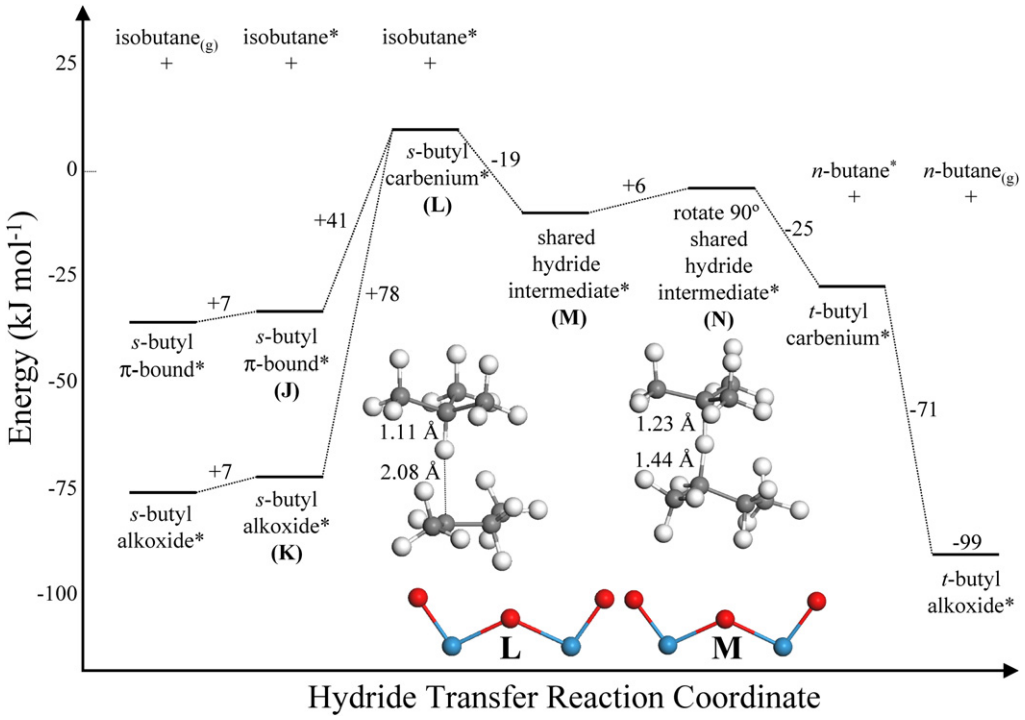

Fig. 5. Reaction energy diagram for hydride transfer from isobutane to an adsorbed *s*-butyl species over HPW. Energies are given relative to separated *trans*-2-butene, isobutane, and $H_3PW_{12}O_{40}$ fragments. Asterisks label surface species. Key structures are illustrated. All structures are illustrated and detailed in supplementary material. All calculations were performed on the full Keggin unit.

indicating that the steric interactions involved in rotation may affect the overall hydride-transfer rate. Because the isobutane-to-*s*-butyl hydride transfer is not symmetric, the completion of the hydride transfer process follows a different route. The final step is dissociation of the shared-hydride intermediate to produce an *n*-butane molecule and a surface *t*-butyl species. This process is unactivated, because rotation of the shared-hydride intermediate to place the *t*-butyl fragment closer to the surface, followed by formation of a *t*-butyl carbenium ion and *n*-butane, are both exothermic steps.

Hydride transfer to a secondary carbon atom has a substantially higher reaction barrier than to a species adsorbed through a tertiary carbon atom. This is due to the decreased stability of the less-substituted secondary carbenium ion transition state compared with the tertiary carbenium ion transition state discussed earlier. Stabilization of the carbenium ions by isobutane in the form of a shared-hydride structure is weak, and thus the driving force for hydride transfer is small. The hydride transfer rate may be expected to be highest over a solid acid that best stabilizes the carbenium-ion transition state. However, the relative rate of the hydride transfer step to the alkylation step controls catalyst deactivation, and stabilization of carbenium ions on the catalyst surface may enhance the alkylation rate as well. The following sections examine the alkylation reaction step to provide relative energies for comparison with hydride transfer.

3.4. HPW-catalyzed alkylation of t-butyl with trans-2-butene

The alkylation of an adsorbed *t*-butyl species with *trans*-2-butene was examined over the O_d–W–O_c region of the HPW Keggin unit for direct comparison with the energies of hydride transfer. The alkylation reaction was assumed to occur through the formation of a complex in which the alkene stabilizes a carbenium ion, followed by the formation of a C–C bond between the two C_4 species. The reaction was considered with the *t*-butyl species initially in an alkoxy or a π-bound state. The final product of the alkylation reaction is a C_8 alkoxide (3,3,4-trimethyl-2-pentyl alkoxide). Fig. 6 illustrates the reaction energy diagram and key structures for *t*-butyl alkylation. The overall reaction energy for the alkylation of the *t*-butyl alkoxide with a gas-phase *trans*-2-butene to form the C_8 alkoxide is -22 kJ mol^{-1}.

Independent of the initial adsorbed state of the *t*-butyl species, the transition state for alkylation is a *t*-butyl carbenium ion interacting weakly with *trans*-2-butene. Carbenium ions have previously been identified as transition states for the alkylation reaction, or its reverse β-scission reaction, over zeolite structures [17,18,53,59]. Carbenium ion formation is stabilized by interaction with the *trans*-2-butene molecule during the alkylation step, as opposed to the hydride transfer reaction, in which the carbenium ion transition state does not interact with isobutane. The activation barrier to alkylation from the alkoxide state is 59 kJ mol^{-1}, and that from the π-bound state is 7 kJ mol^{-1}. The stabilized carbenium intermediate structure (**R**) is slightly more stable than the carbenium ion transition state, and the energy of stabilization ($E_{\text{stabilization}}$) is -9 kJ mol^{-1}. Completion of the alkylation reaction occurs through formation of a C–C bond between the two C_4 fragments [C(3)–C(4) in Fig. 6]. The transition state for conversion of the stabilized intermediate (**R**) to a C_8 alkoxide is a secondary carbenium ion (**S**), with

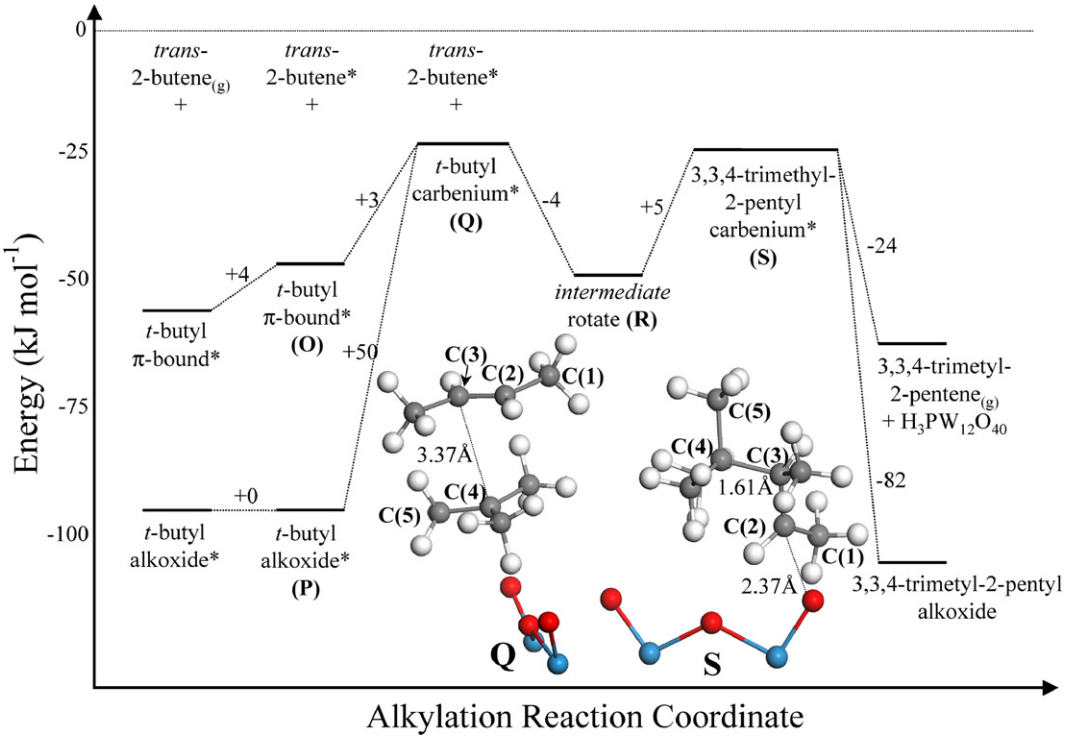

Fig. 6. Reaction energy diagram for alkylation of an adsorbed *t*-butyl species with *trans*-2-butene over HPW. Energies are given relative to separated isobutene, *trans*-2-butene, and $H_3PW_{12}O_{40}$ fragments. Asterisks label surface species. Key structures are illustrated. All structures are illustrated and detailed in supplementary material. All calculations were performed on the full Keggin unit.

the positive charge formally on the C(2) carbon. This transition state (**S**) is slightly more stable than the tertiary carbenium ion (**Q**) due to the exothermic formation of the C–C bond. Although our calculations explicitly considered only the alkoxide as the final product of alkylation, direct deprotonation from the transition state **S** can also generate a π-bound C_8 adsorbate, which may desorb as 3,3,4-trimethyl-2-pentene. As illustrated in Fig. 6, the alkoxide is more stable than the alkene product, as alkene adsorption is exothermic over HPW. The reaction of an adsorbed *t*-butyl species and gas-phase *trans*-2-butene molecule to form 3,3,4-trimethyl-2-pentene is exothermic by -16 kJ mol^{-1} with *t*-butyl initially in the π-bound state and endothermic by 36 kJ mol^{-1} with *t*-butyl initially in the alkoxy state.

3.5. HPW-catalyzed alkylation of s-butyl with trans-2-butene

The alkylation of an adsorbed *s*-butyl species with *trans*-2-butene was also considered over the O_d–W–O_c region of the HPW Keggin. The adsorption of a *trans*-2-butene molecule to form an adsorbed *s*-butyl species was reported previously [41]; therefore, this step completes the reaction mechanism of *trans*-2-butene oligomerization and also represents a step in the overall alkylation mechanism. Fig. 7 illustrates the energetics and key structures for this reaction. The overall reaction energy for converting an *s*-butyl alkoxide to a C_8 alkoxide (3,4-dimethyl-2-hexyl alkoxide) is -36 kJ mol^{-1}. The overall activation barrier to alkylation from the alkoxide state is 78 kJ mol^{-1} and from the π-bound state is 30 kJ mol^{-1}. The transition state for conversion of *s*-butyl is again a secondary carbenium ion; however, *trans*-2-butene substantially stabilizes the carbenium ion transition states to alkylation. The transition state from the alkoxide (**V**) is stabilized by -13 kJ mol^{-1} with respect to the *s*-butyl carbenium ion transition state to *trans*-2-butene adsorption. The transition state for alkylation directly from the π-bound state (**W**) is further stabilized due to the closer approach of *trans*-2-butene, reducing the activation barrier to carbenium ion formation and subsequent alkylation. Alkylation from the π-bound state occurs in a concerted manner, with proton donation from the acid occurring as a carbon atom [C(4)] of the *s*-butyl species interacting with the electron density of the *trans*-2-butene C=C double bond.

After formation of a stabilized carbenium intermediate, formation of the C_8 alkoxide occurs through a secondary carbenium ion [positive charge formally on a C(2) atom labeled in Fig. 7]. However, this carbenium ion is of lower energy than the stabilized intermediate due to the exothermic C–C bond formation and thus does not represent an extremum within the reaction scheme. Direct deprotonation of the C_8 carbenium ion produces a π-bound 3,4-dimethyl-2-hexyl species that can subsequently desorb as 3,4-dimethyl-2-hexene, completing butene oligomerization. The concerted pathway to oligomerization directly from the *s*-butyl π-bound state occurs with an overall barrier of 30 kJ mol^{-1} and an overall oligomerization energy of -31 kJ mol^{-1} from the π-bound state or -69 kJ mol^{-1} from two gas-phase *trans*-2-butene molecules. Because the single-step concerted pathway to oligomerization never forms an alkoxide, alkene oligomerization may continue occurring on sites that sterically hinder alkoxide formation.

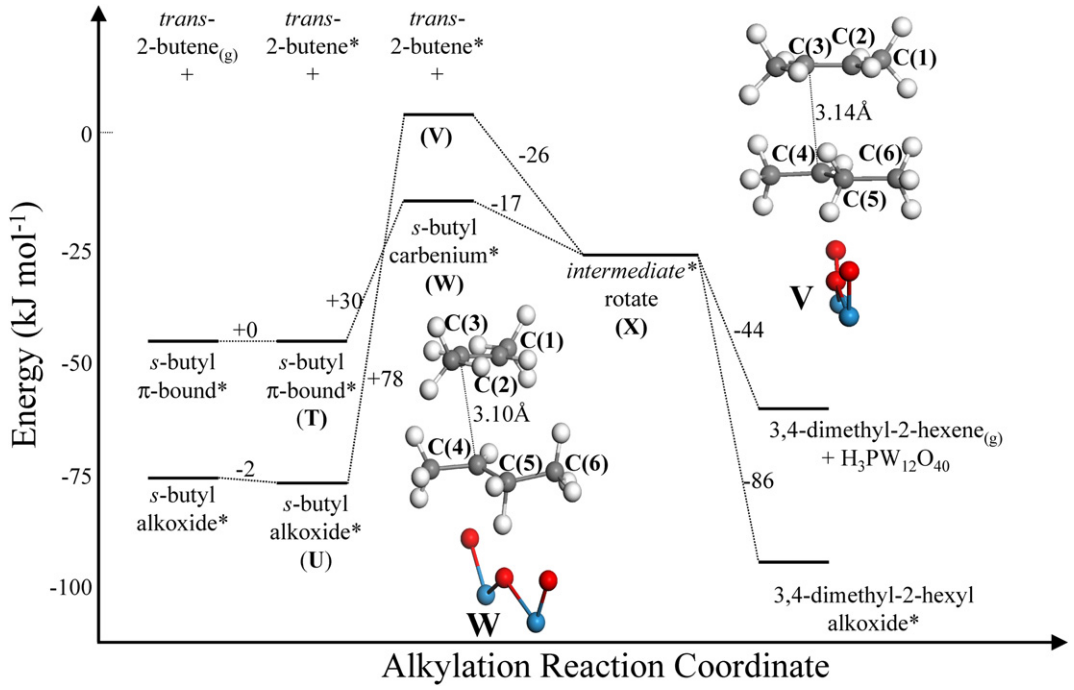

Fig. 7. Reaction energy diagram for alkylation of an adsorbed *s*-butyl species with *trans*-2-butene over HPW. Energies are given relative to separated *trans*-2-butene, *trans*-2-butene, and $H_3PW_{12}O_{40}$ fragments. Asterisks label surface species. Key structures are illustrated. All structures are illustrated and detailed in supplementary material. All calculations were performed on the full Keggin unit.

Table 2
Overall energetics of hydride transfer and alkylation over phosphotungstic acid[a]

	ΔE_{rxn} alkoxide to alkoxide	E_{act}	
		From alkoxide	From π-bound
Hydride transfer: isobutane to *t*-butyl	0	69	28
Alkylation: *trans*-2-butene to *t*-butyl	−22	59	7
Hydride transfer: isobutane to *s*-butyl	−14	85	48
Alkylation: *trans*-2-butene to *s*-butyl	−36	78	30

[a] All energies in kJ mol^{-1}.

3.6. Comparison of relative barriers

Table 2 summarizes the reaction energetics for hydride transfer and alkylation over phosphotungstic acid. The alkylation reaction is more exothermic than hydride transfer for both *t*-butyl and *s*-butyl intermediates. Furthermore, alkylation has a lower activation barrier than hydride transfer in all cases due to the stabilization of the carbenium ion transition states by the *trans*-2-butene reactant, in contrast to the lack of stabilization by isobutane in hydride transfer. The barriers for both hydride transfer and alkylation are lower for reaction with a *t*-butyl intermediate than for reaction with a *s*-butyl intermediate. This is due to the enhanced stability of the tertiary carbenium ion transition state over that of the secondary state. However, the presence of an electron-donating alkene stabilizes the secondary carbenium ion, thus making the alkylation of *s*-butyl (or, more generally, alkyl species adsorbed through an unsaturated secondary carbon atom) highly favored over hydride transfer.

Experimental measurements of activation barriers for these steps over phosphotungstic acid are not available. Simpson et al. fit a simplified model of the alkylation mechanism to initial reaction rate data to determine the intrinsic relative rate of alkylation and hydride transfer over an ultrastable Y-type zeolite [6]. The ratio of the rate constant of alkylation to that of hydride transfer was found to be 8000 at 323 K and 3800 at 373 K, yielding an activation barrier for alkylation that is 14.9 kJ mol^{-1} lower than that for hydride transfer and a pre-exponential factor for alkylation that is 30 times greater than that for hydride transfer. Our calculations show that the activation barrier for alkylation of a *t*-butyl alkoxide was 10 kJ mol^{-1} lower than that for hydride transfer, in good agreement with the experimental results over zeolite catalysts [6]. As shown in Figs. 2 and 3, the interaction of a carbenium ion with an alkene is substantially longer-range than the interaction with an alkane. Thus, the pre-exponential factor for alkylation would be expected to be greater for the alkylation step, because an encounter between an alkene and a carbenium ion is likely to show a greater sticking coefficient than an encounter between an alkane and a carbenium ion.

The relative rates presented herein allow comparison of the energies of alkene oligomerization and alkylation over phosphotungstic acid. During the alkylation reaction. selectivity to alkanes decreases at long times on stream, with only alkene oligomerization continuing on the deactivated catalyst [2,6,7,12,13]. Furthermore, alkene oligomerization may produce heavy hydrocarbon species that block catalyst pores and acid

sites. Alkene oligomerization occurs through successive alkylation steps, producing higher alkene products without participating in hydride transfer. In the alkylation mechanism, isobutane enters only through a hydride-transfer step, which has a higher barrier than oligomerization.

Carbenium ion stability relative to the adsorbed state, is the controlling factor in the performance of an acid catalyst for alkylation. Increasing carbenium ion stability reduces the barriers to both the alkylation and hydride-transfer steps, thereby increasing the rates within the propagation cycle. Furthermore, carbenium ion stability is expected to correlate with selectivity to hydride transfer versus overalkylation or alkene oligomerization. The better the catalyst surface is in stabilizing the carbenium ion transition state, the lower the differential stabilizing effect between alkanes and alkenes. As shown previously, the interaction energy of the carbenium ion with an alkane or alkene is substantially decreased over the HPA surface due to stabilization by the catalyst conjugate anion. The interaction energy with the alkane or alkene scales inversely with the interaction energy with the surface, suggesting that greater stabilization by the surface will lead to a decreased differential stabilization between alkanes and alkenes.

It is not surprising that all of the Brønsted acid catalysts used for the alkylation of isobutane with *trans*-2-butene deactivate through the buildup of heavy hydrocarbons. In fact, heavy hydrocarbons form with both homogeneous and heterogeneous acid catalysts. In the case of homogeneous catalysts, the acid-soluble oil, referred to as "red oil," is separated from the useful product, and the entrapped catalyst is worked up externally [2, 11]. A zeolite alkylation catalyst was recently commercialized; in this process, the local concentration of alkene is carefully controlled throughout the reactor and the catalyst is regenerated off-line every 1–3 h [9].

Heteropolyacids are less thermally stable than zeolite catalysts, and thus are not likely to be viable alternatives in processes requiring high-temperature regeneration. As long as alkylation and hydride transfer share a common carbenium ion transition state, the hydride transfer reaction is expected to have a substantially lower rate constant. Design of a solid acid catalyst should include structures that best stabilize carbenium ion transition states relative to adsorbed states or facilitate hydride transfer reactions through an alternative reaction mechanism.

4. Conclusion

DFT calculations suggest that hydride transfer from isobutane to an adsorbed alkyl intermediate on the surface of phosphotungstic acid proceeds via formation of a surface carbenium ion transition state and subsequent complexation of the carbenium ion with isobutane to form a shared-hydride intermediate. Thus, the overall barrier to hydride transfer is the energy required to convert the adsorbed alkyl species to a carbenium ion. Formation of the carbenium ion from alkoxide or π-bound adsorbed states is not affected by the presence of isobutane. Hydride transfer to a tertiary carbon atom occurs with a substantially lower barrier than transfer to a secondary carbon atom because of the greater stability of the more substituted carbenium ion. Alkylation of an adsorbed alkyl species also proceeds through a carbenium ion transition state; however, the transition state for alkylation is stabilized by interaction with the alkylating alkene. These findings suggest that alkylation proceeds with an intrinsically lower reaction barrier than hydride transfer, leading to the buildup of heavy hydrocarbons and catalyst deactivation.

Acknowledgments

This work was funded by the National Science Foundation (CTS-0124333). Part of the research was performed using the Molecular Science Computing Facility (MSCF) in the William R. Wiley Environmental Molecular Sciences Laboratory, a national scientific user facility sponsored by the U.S. Department of Energy's Office of Biological and Environmental Research and located at the Pacific Northwest National Laboratory. Pacific Northwest is operated for the Department of Energy by Battelle.

Supplementary material

Charge analysis of gas-phase hydride transfer and alkylation intermediates, structural figures of all equilibrium and transition states referenced in Figs. 3–7, as well as key interatomic distances and angles.

Please visit doi: 10.1016/j.jcat.2006.08.013.

References

[1] J. Weitkamp, Y. Traa, in: G. Ertl, H. Knozinger, J. Weitkamp (Eds.), Handbook of Heterogeneous Catalysis, vol. 4, VCH, Weinheim, 1997, pp. 2039–2069.
[2] J. Weitkamp, Y. Traa, Catal. Today 49 (1999) 193.
[3] S.I. Hommeltoft, Appl. Catal. A 221 (2001) 421.
[4] J. Stell, Oil Gas J. 101 (2003) 68.
[5] M. Guisnet, N.S. Gnep, Appl. Catal. A 146 (1996) 33.
[6] M.F. Simpson, J. Wei, S. Sundaresan, Ind. Eng. Chem. Res. 35 (1996) 3861.
[7] K.P. de Jong, C.M.A.M. Mesters, D.G.R. Peferoen, P.T.M. van Brugge, C. de Groot, Chem. Eng. Sci. 51 (1996) 2053.
[8] C.A. Querini, Catal. Today 62 (2000) 135.
[9] R.L. D'Aquino, Chem. Eng. Prog. 101 (2005) 10.
[10] J.A. Lercher, A. Feller, S. Gaab, PCT. Int. Appl. Patent # WO02094436 (2002).
[11] A. Corma, A. Martinez, Catal. Rev.-Sci. Eng. 35 (1993) 483.
[12] K. Yoo, P.G. Smirniotis, Appl. Catal. A Gen. 246 (2003) 243.
[13] A. Feller, A. Guzman, I. Zuazo, J.A. Lercher, J. Catal. 224 (2004) 80.
[14] F. Cardona, N.S. Gnep, M. Guisnet, G. Szabo, P. Nascimento, Appl. Catal. A Gen. 128 (1995) 243.
[15] A. Feller, I. Zuazo, A. Guzman, J.O. Barth, J.A. Lercher, J. Catal. 216 (2003) 313.
[16] A. Platon, W.J. Thomson, Appl. Catal. A Gen. 282 (2005) 93.
[17] V.B. Kazansky, Catal. Today 51 (1999) 419.
[18] A.M. Rigby, G.J. Kramer, R.A. van Santen, J. Catal. 171 (1997) 1.
[19] J.F. Haw, B.R. Richardson, I.S. Oshiro, N.D. Lazo, J.A. Speed, J. Am. Chem. Soc. 111 (1989) 2052.
[20] E.G. Derouane, H. He, S.B. Derouane-Abd Hamid, I.I. Ivanova, Catal. Lett. 58 (1999) 1.
[21] V.B. Kazansky, I.N. Senchenya, J. Mol. Catal. 74 (1992) 257.
[22] P.E. Sinclair, A. de Vries, P. Sherwood, C.R.A. Catlow, R.A. van Santen, J. Chem. Soc. Faraday Trans. 94 (1998) 3401.

[23] A. Bhan, Y.V. Joshi, W.N. Delgass, K.T. Thomson, J. Phys. Chem. B 107 (2003) 10476.
[24] X. Rozanska, T. Demuth, F. Hutschka, J. Hafner, R.A. van Santen, J. Phys. Chem. B 106 (2002) 3248.
[25] X. Rozanska, R.A. van Santen, T. Demuth, F. Hutschka, J. Hafner, J. Phys. Chem. B 107 (2003) 1309.
[26] P. Viruela-Martin, C.M. Zicovich-Wilson, A. Corma, J. Phys. Chem. 97 (1993) 13713.
[27] V.B. Kazansky, M.V. Frash, R.A. van Santen, Appl. Catal. A 146 (1996) 225.
[28] M.V. Frash, V.B. Kazansky, A.M. Rigby, R.A. van Santen, J. Phys. Chem. B 102 (1998) 2232.
[29] V.B. Kazansky, M.V. Frash, R.A. van Santen, Stud. Surf. Sci. Catal. 105 (1997) 2283.
[30] M. Boronat, P. Viruela, A. Corma, J. Phys. Chem. A 102 (1998) 9863.
[31] M. Boronat, C.M. Zicovich-Wilson, A. Corma, P. Viruela, Phys. Chem. Chem. Phys. 1 (1999) 537.
[32] K. Yoo, E.C. Burckle, P.G. Smirniotis, J. Catal. 211 (2002) 6.
[33] V.B. Kazansky, Appl. Catal. A Gen. 188 (1999) 121.
[34] S.I. Hommeltoft, O. Ekelund, J. Zavilla, Ind. Eng. Chem. Res. 36 (1997) 3491.
[35] T. Okuhara, T. Nishimura, H. Watanabe, M. Misono, J. Mol. Catal. 74 (1992) 247.
[36] R.S. Drago, J.A. Dias, T.O. Maier, J. Am. Chem. Soc. 119 (1997) 7702.
[37] T. Blasco, A. Corma, A. Martinez, P. Martinez-Escolano, J. Catal. 177 (1998) 306.
[38] W. Chu, Z. Zhao, W. Sun, X. Ye, Y. Wu, Catal. Lett. 55 (1998) 57.
[39] N. Essayem, S. Kieger, G. Coudurier, J.C. Vedrine, Stud. Surf. Sci. Catal. 101 (1996) 591.
[40] P.Y. Gayraud, I.H. Stewart, S.B. Derouane-Abd. Hamid, N. Essayem, E.G. Derouane, J.C. Vedrine, Catal. Today 63 (2000) 223.
[41] K.A. Campbell, M.J. Janik, M. Neurock, R.J. Davis, Langmuir 21 (2004) 4738.
[42] M.J. Janik, R.J. Davis, M. Neurock, Catal. Today 105 (2005) 134.
[43] M.J. Janik, R.J. Davis, M. Neurock, Catal. Today 116 (2006) 90.
[44] G. Kresse, J. Hafner, Phys. Rev. B 47 (1993) 558.
[45] G. Kresse, J. Furthmuller, Comput. Mater. Sci. 6 (1996) 15.
[46] G. Kresse, J. Furthmuller, Phys. Rev. B 54 (1996) 11169.
[47] D. Vanderbilt, Phys. Rev. B 41 (1990) 7892.
[48] J.P. Perdew, J.A. Chevary, S.H. Vosko, K.A. Jackson, M.R. Pederson, D.J. Singh, C. Fiolhais, Phys. Rev. B 46 (1992) 6671.
[49] H.J. Monkhorst, J.D. Pack, Phys. Rev. B 13 (1976) 5188.
[50] M.J. Janik, K.A. Campbell, B.B. Bardin, R.J. Davis, M. Neurock, Appl. Catal. A 256 (2003) 51.
[51] G. Mills, H. Jonsson, G.K. Schenter, Surf. Sci. 324 (1995) 305.
[52] J. Eckert, T.D. Sewell, J.D. Kress, E.M. Kober, L.L. Wang, G. Olah, J. Phys. Chem. A 108 (2004) 11369.
[53] S. Svelle, S. Kolboe, O. Swang, J. Phys. Chem. B 108 (2004) 2953.
[54] G. Fu, X. Xu, X. Lu, H. Wan, J. Phys. Chem. B 109 (2005) 6416.
[55] I. Milas, M.A.C. Nascimento, Chem. Phys. Lett. 338 (2001) 67.
[56] M. Boronat, P. Viruela, A. Corma, J. Phys. Chem. B 103 (1999) 7809.
[57] M. Boronat, P. Viruela, A. Corma, J. Phys. Chem. B 101 (1997) 10069.
[58] D. Farcasiu, P. Lukinskas, Phys. Chem. Chem. Phys. 2 (2000) 2373.
[59] P.J. Hay, A. Redondo, Y. Guo, Catal. Today 50 (1999) 517.